Environ. Sci. Technol. **2001**, *35,* 4773−4782

Partitioning of Total Mercury and Methylmercury to the Colloidal Phase in Freshwaters

CHRISTOPHER L. BABIARZ,*,† JAMES P. HURLEY,‡,§ STEPHEN R. HOFFMANN,† ANDERS W. ANDREN,† MARTIN M. SHAFER,† AND DAVID E. ARMSTRONG†

Environmental Chemistry and Technology Program, University of Wisconsin—Madison, 660 North Park Street, Madison, Wisconsin 53706-1484, Bureau of Integrated Science Services, Wisconsin Department of Natural Resources, 1350 Femrite Drive, Monona, Wisconsin 53716, and Water Resources Institute, University of Wisconsin—Madison, 1975 Willow Drive, Madison, Wisconsin 53706.

Using tangential flow ultrafiltration, total mercury (Hg_T) and methylmercury (MeHg) concentrations in the colloidal phase (0.4 μm−10 kDa) were determined for 15 freshwaters located in the upper Midwest (Minnesota, Michigan, and Wisconsin) and the Southern United States (Georgia and Florida). Unfiltered concentrations were typical of those reported for freshwater and ranged from 0.9 to 27.1 ng L^{-1} Hg_T and from 0.08 to 0.86 ng L^{-1} MeHg. For some rivers, Hg_T and MeHg in the colloidal phase comprised up to 72% of the respective unfiltered concentration. On average, however, Hg_T and MeHg concentrations were evenly distributed between the particulate (>0.4 μm), colloidal, and dissolved (<10 kDa) phases. The pool of Hg in the colloidal phase decreased with increasing specific conductance. Results from experiments on freshwaters with artificially elevated specific conductance suggest that Hg_T and MeHg may partition to different subfractions of colloidal material. The colloidal-phase Hg_T correlation with filtered organic carbon (OC_F) was generally poor (r^2 < 0.14; p > 0.07), but the regression of MeHg with OC_F was strong, especially in the upper Midwest (r^2 = 0.78; p < 0.01). On a mass basis, colloidal-phase Hg concentrations were similar to those of unimpacted sediments in the Midwest. Mercury to carbon ratios averaged 352 pg of Hg_T/mg of C and 25 pg of MeHg/mg of C and were not correlated to ionic strength. The log of the partition coefficient (log K_D) for Hg_T and MeHg ranged from 3.7 to 6.4 and was typical of freshwater values determined using a 0.4 μm cutoff between the particulate phase and the dissolved phase. Log K_D calculated using the <10 kDa fraction as "dissolved" ranged from 4.3 to 6.6 and had a smaller standard deviation about the mean. In addition, our data support the "particle concentration effect" (PCE) hypothesis that the association of Hg with colloids in the filter-passing fraction can lower the observed log K_D. The similarity between colloidal and particulate-phase partition coefficients suggests that colloidal mass and not preferential colloidal partitioning drives the PCE.

* Corresponding author e-mail: babiarz@cae.wisc.edu; phone: (608)265-5085; fax: (608)262-0454.

† Environmental Chemistry and Technology Program, University of Wisconsin—Madison.

‡ Wisconsin Department of Natural Resources.

§ Water Resources Institute, University of Wisconsin—Madison.

Introduction

The distribution of mercury (Hg) species between the particulate, colloidal, and dissolved phase affects the toxicity, transport, and biouptake of Hg in freshwaters (*1*−*3*). Among these size classes, the colloidal phase has been inferred to play several key roles in the biogeochemistry of Hg. First, colloids may play an important role in regulating the concentration of dissolved metal ion and neutral complexes in solution (*4*). The binding of free metal ion reduces acute toxicity, and regulating neutral complexes may affect Hg transport across bacterial walls (*5*)—notable because sulfur-reducing bacteria have been shown to convert inorganic Hg into the bioaccumulative methyl form through a detoxification response (*6*, *7*). Second, colloids may be an important downstream transport vector due to the relatively large surface area of colloids and the well-known particle-reactive nature of Hg. Finally, the concentration and chemical character of colloids may affect the uptake of methylmercury (MeHg) by bacteria, fungi, zooplankton, and mollusks either by direct consumption or the free ion activity model (*3*, *8*, *9*).

Unfortunately, the role of the colloidal phase in the biogeochemistry of Hg has been largely left to inference; there are few direct measurements of Hg associated with either colloidal-sized particles (roughly 0.4 μm−10 kilodalton (kDa)) or the "dissolved" phase (<10 kDa) because methods to cleanly isolate colloidal material have been only recently evaluated for trace-level Hg research within marine waters (*10*) and freshwaters (*11*).

Most measurements of colloidal-phase Hg in natural waters originate from coastal marine environments and focus largely on total mercury (Hg_T). One of these studies reported the first colloidal-phase Hg_T data from deep Pacific Ocean waters (*10*), and two others applied tangential-flow ultrafiltration to three Texas estuaries (*12*, *13*). The last two documented non-conservative mixing of colloidal-phase Hg along a salinity gradient from the freshwater Trinity River to the saline Galveston Bay. They found that a major portion of the filtered fraction (12−93%) was associated with the 0.4 μm−1 kDa size fraction and that the colloidal-phase Hg_T concentration was correlated with carbon content. In addition, colloid coagulation in these high salinity waters was shown to be a major removal mechanism for Hg_T.

Another study in the Ochlockonee River Estuary of Florida concurred that Hg_T in the 0.4 μm−1 kDa fraction was a large portion of the filtered phase (37−88%) in coastal marine environments (*14*). They showed that 5−50% of dissolved Hg_T in the Atlantic Ocean was in the 0.4 μm−1 kDa pool. They also presented evidence that thiol functional groups associated with organic carbon were important in the partitioning of Hg_T in the colloidal phase. In addition, they reported the first colloidal-phase MeHg concentrations in marine environments.

The phase distribution of both Hg_T and MeHg in freshwaters may differ from that in marine environments because freshwaters are in general lower in ionic strength, higher in alkalinity, and higher in dissolved organic carbon (DOC). A Florida study presented the first colloidal-phase MeHg data in freshwater (*15*), stating that 43−70% of the MeHg in the filtered fraction was found in the 0.22 μm−3

10.1021/es010895v CCC: $20.00
Published on Web 11/10/2001

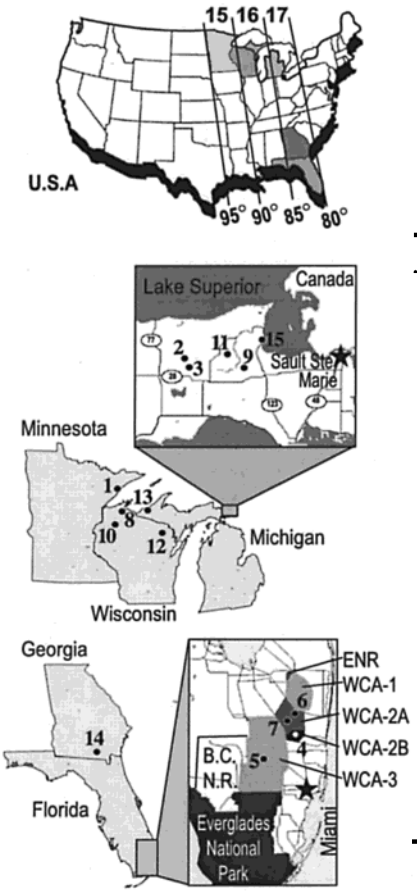

Site Location

Universal Transverse Mercator Coordinates*

#	Site Name	Zone	North (m)	West (m)
1	Baptism River	15	5,244,275	635,900
2	East Creek (headwater)	16	5,138,850	599,400
3	East Creek (wetland)	16	5,135,450	599,800
4	Everglades (2B South)	17	2,893,975	562,150
5	Everglades (3A15)	17	2,873,950	533,075
6	Everglades (F1)	17	2,915,525	562,750
7	Everglades (U3)	17	2,907,675	558,800
8	Fish Creek	15	5,160,375	655,825
9	Hendrie Creek	16	5,130,850	638,950
10	Moose River	15	5,098,300	656,300
11	Murphy Creek	16	5,147,450	620,550
12	Popple River	16	5,072,900	363,475
13	Presque Isle River	16	5,175,350	272,550
14	Suwanee River	17	3,408,700	364,400
15	Tahquamenon River	16	5,157,700	650,400

North American Datum 1983 (NAD83)

FIGURE 1. Location of the freshwaters studied. On the Everglades inset map, ENR, WCA, and BCNR stand for Everglades Nutrient Removal Area, Water Conservation Area, and Big Cypress National Reserve, respectively. Everglades sites 4, 5, and 6/7 are located within Water Conservation Areas 2B, 3A, and 2A, respectively.

kDa fraction. In addition, the colloidal-phase Hg_T and MeHg concentrations in the Everglades appeared strongly correlated with organic carbon.

These previous studies have established a strong foundation on colloidal Hg_T dynamics in coastal marine environments, have presented the first data on colloidal-phase Hg_T and MeHg in the open oceans, and have initiated a pilot study of colloidal-phase Hg_T and MeHg in the freshwaters of the Everglades. Before detailed process-oriented questions can be thoroughly addressed, additional information on Hg in the colloidal phase is needed from both deep ocean waters and geochemically distinct freshwaters. Noticeably absent is colloidal-phase Hg information from waters of low ionic strength ($<400\ \mu S\ cm^{-1}$) and of differing DOC character.

We have previously shown that tangential-flow ultrafiltration is an effective tool for isolating colloids in freshwaters using trace-level clean techniques (*11*, *16*). In this paper, we contrast geochemical characteristics of rivers in the upper Midwest, Georgia, and the Florida Everglades to explore the effects of ionic strength and organic carbon on the colloidal-phase partitioning of Hg. In addition, the influence of the colloidal phase on estimates of the partition coefficient (K_D) is examined within the context of the particle concentration effect (PCE). The PCE hypothesis states that the presence of colloids under high particulate loading leads to low estimates of K_D—important because underestimates of K_D may lead to biased conclusions drawn from partitioning models. Together, all these contributions help establish a description of the geochemical factors that support colloidal-phase partitioning of Hg in freshwaters.

Materials and Methods

Fifteen freshwaters (Figure 1) were examined to measure colloidal-phase partitioning of Hg_T and MeHg. The waters were selected to provide a broad range of water chemistry conditions including pH, DOC, suspended particulate matter (SPM), and specific conductance (Table 1). Ten sites were grouped in Midwestern states of Michigan, Minnesota, and Wisconsin; four sites were in the Florida Everglades; and one site was in Georgia (the Suwanee River). Whole-water samples were filtered in-line using conventional 0.4 μm Meissner filtration capsules (0.22 μm Calyx capsules in 1996) equipped with an all-Teflon sampling line and weight. Conventional filtrates were further processed using 10 kDa (approximately 0.0015 μm) ultrafiltration to isolate the colloidal and dissolved phases.

Ultrafiltration separations were usually performed within 6−12 h after collection using 0.23 m^2 spiral-wound regenerated cellulose membranes (Millipore model PLGC). A few comparative separations were performed on polyethersulfone membranes (PTGC). The average elapsed time before processing by ultrafiltration was 8.8 h ($s = 3.8$; $n = 21$). Samples were kept at ambient temperature to minimize equilibrium shifts. All sample containers, tubing, and pump heads were composed of Teflon. An exhaustive, multiple-step cleaning process was employed to prepare the cartridges for trace metal applications (*11*, *16*).

During an ultrafiltration separation, the membrane-passing fraction (permeate) was collected at a rate of 20−30 mL min^{-1}. The nonpassing fraction (retentate) was recirculated until the ratio of the retentate volume to the feed volume (concentration factor) was about 8:1. The concen-

TABLE 1. Water Chemistry Parameters of the Sampling Sites

name	date	pH	specific conductance (μS cm^{-1})	suspended particulate matter (mg L^{-1})	colloidal phase[a] (0.4 μm−10 kDa) OC$_C$ (mg L^{-1})	Al$_C$ (μg L^{-1})	Fe$_C$ (μg L^{-1})	total colloid[b] (0.4 μm−10 kDa) (mg L^{-1})	SD	% OC[c]
Baptism River	Mar 1998	7.3	48.8	6.2	7.7	163.0	276.0	17.4	0.03	88.3
Baptism River	Jul 1998	8.2	118.2	0.5	3.4	9.0	66.0	7.0	0.19	97.3
Baptism River	Oct 1998	7.0	49.3	5.3	13.5	126.4	360.0	28.9	0.78	93.7
East Creek (headwater)	Aug 1997	7.6	131.0	1.7	0.4	1.5	9.5	0.8	0.05	96.5
East Creek (wetland)	Aug 1997	~7	110.0	0.4	6.4	7.0	95.0	12.9	0.53	98.4
Everglades (2B south)	Jul 1997	7.3	443.0	7.3	4.5	1.8	60.0	9.2	0.08	98.8
Everglades (3A15)	Jul 1997	7.0	239.0	0.8	3.5	0.0	88.0	7.2	0.21	98.2
Everglades (F1)	Jul 1997	7.3	1072.0	1.0	6.6	4.1	12.0	13.4	0.32	99.6
Everglades (U3)	Jul 1997	7.7	1189.0	0.7	8.6	0.0	29.0	17.2	0.27	99.7
Fish Creek	Oct 1997	8.0	157.0	4.6	0.2	15.2	34.8	0.6	0.09	65.1
Fish Creek	Mar 1998	7.5	100.4	236.0	6.9	1098.0	866.0	26.1	0.50	52.9
Fish Creek	Jun 1998	7.9	174.0	49.5	1.5	180.6	151.0	5.0	0.09	59.3
Hendrie Creek	Aug 1997	7.6	223.0	5.4	2.6	7.3	969.0	6.8	0.19	77.6
Moose River[d]	Aug 1996	6.4	41.9	10.9	26.5	193.0	2432.0	58.5	0.34	90.5
Murphy Creek	Aug 1997	7.2	149.4	4.3	2.8	19.3	3636.0	11.3	0.75	50.0
Popple River[d]	Aug 1996	6.5	81.6	1.6	21.7	39.0	753.0	44.9	1.20	96.6
Presque Isle River	Apr 1998	7.0	30.7	13.5	9.2	112.0	157.0	19.7	0.23	93.1
Presque Isle River	Jul 1998	8.0	156.0	1.0	3.0	1.5	28.0	6.0	0.18	99.0
Presque Isle River	Oct 1998	7.5	133.6	3.1	4.8	11.1	119.8	9.8	0.09	97.0
Suwanee River	Jul 1997	3.8	86.0	1.1	23.0	375.5	814.0	50.9	1.33	90.2
Tahquamenon River	Apr 1998	7.1	57.1	8.6	7.7	65.5	193.0	16.3	0.22	94.2
Tahquamenon River	Jun 1998	7.8	137.4	4.4	3.5	16.1	183.3	7.5	0.34	94.2
Tahquamenon River	Oct 1998	7.5	164.0	1.6	4.0	19.9	302.3	8.7	0.31	92.5
	mean	7.2	221.4	16.1	7.5	107.2	505.9	16.8	0.36	87.9
	SD	0.9	300.1	49.0	7.2	235.0	869.3	15.5	0.35	15.6
	median	7.4	133.6	4.3	4.8	16.1	157.0	11.3	0.23	94.2
	min	3.8	30.7	0.4	0.2	0.0	9.5	0.6	0.03	50.0
	max	8.2	1189.0	236.0	26.5	1098.0	3636.0	58.5	1.33	99.7

[a] Used to estimate the total colloid mass for the calculation of partition coefficients. [b] Total colloid = 2[OC$_C$] + 10[Al$_C$] + 1.5[Fe$_C$]. [c] % OC = 2[OC$_C$] ÷ [total colloid]. [d] The measured colloidal phase was 0.22 μm−10 kDa on sampling dates in 1996.

tration factor was kept below 10 to avoid changes in equilibrium metal partitioning to organic carbon (*10*, *17*). A mass balance was conducted with each separation as part of the QA/QC protocol. Mass balance closure was calculated from the following fractions: (1) the feed solution, (2) the preconditioning solution (sampled after the preconditioning step was completed), (3) the final retentate, (4) several permeate subsamples, (5) a post-separation Milli-Q flush, and (6) a dilute sodium hydroxide rinse (0.1 N).

In general, freshwaters with small colloidal loads (<2 mg L^{-1}) tested the limits of our ultrafiltration protocol because Hg concentrations were also low (<1 ng L^{-1} Hg$_T$). Using larger feed volumes (>5 L) could improve the relative error. Mercury mass balance results were generally excellent, averaging 104.8% (SD = 13.6) for Hg$_T$ and 101.3% (SD = 11.5) for MeHg (Table 2). These error terms are comparable to our laboratory analytical protocols that require the reanalysis of individual samples until the relative standard deviation is within 10% and spike recoveries are within 25%.

At two sites, the specific conductance of ambient river water was elevated before the ultrafiltration separation to examine the effects of ionic strength on partitioning. A 15 L sample of water from the wetland-influenced East Creek (110 μS cm^{-1}) was spiked with Hg^{2+} and MeHg, homogenized, and split into three 5 L portions. The specific conductance of two portions was elevated with $Ca(NO_3)_2$ to 305 and 670 μS cm^{-1}, shaken, and allowed to equilibrate 1 h before processing under standard protocol. The experiment was repeated with water from the Popple River (60 μS cm^{-1}) that was elevated to 480 μS cm^{-1} by adding $NaNO_3$ but was not spiked with additional Hg.

Total mercury analysis was performed using the bromine monochloride oxidation technique followed by stannous chloride reduction, nitrogen purging, gold-trap preconcentration, thermal desorption, and cold-vapor atomic fluorescence spectroscopy (CVAFS) detection (*18*, *19*). MeHg was determined by distillation, aqueous-phase ethylation, nitrogen purging, Carbotrap preconcentration, thermal desorption, chromatographic separation, pyrolytic conversion to Hg^0, and CVAFS detection (*20*, *21*). The NaOH rinse samples were neutralized with trace metal grade HCl before the distillation. Analytical detection limits (three times the SD of the blank) averaged 0.1 ng L^{-1} Hg$_T$ and 0.02 ng L^{-1} MeHg.

Iron was determined by graphite furnace atomic absorption spectroscopy. The uncertainty in the analytical precision was typically less than 7%, but below 200 μg L^{-1} the uncertainty was driven by the error in the blank (± 7 μg L^{-1}). Aluminum was determined by inductively coupled plasma mass spectrometry (ICPMS) with analytical uncertainty typically less than 5% (or ±0.15 μg L^{-1} if the Al concentration was below 5 μg L^{-1}). Dissolved organic carbon was determined on a Shimadzu TOC-5000 using high-temperature (680 °C) catalytic oxidation. Samples for organic carbon were kept frozen until analysis, and analytical uncertainty was usually ±0.1 mg L^{-1}. In the remainder of this text, we refer to organic carbon in the <0.4 μm fraction as OC$_F$, in the <0.4 μm−10 kDa fraction as OC$_C$, and in the <10 kDa fraction as OC$_D$. The total concentration of colloidal material presented in Table 1 was estimated using the following method (*22*, *23*):

$$C_{TC} = 2C_{OC} + 1.5C_{Fe} + 10C_{Al} \quad (1)$$

where C_{TC} is the total colloid concentration (kg L^{-1}), and C_{OC}, C_{Fe}, and C_{Al} are the organic carbon, iron, and aluminum concentrations in the colloidal phase. Although direct measurement of colloidal mass is preferable, this method

TABLE 2. Total Mercury and Methylmercury as a Percentage of the Unfiltered Value

	total mercury								methylmercury							
			particulate[a] >0.4 μm		colloidal 0.4 μm–10 kDa		dissolved <10 kDa				particulate >0.4 μm		colloidal 0.4 μm–10 kDa		dissolved <10 kDa	
name	unfiltered (ng L^{-1})	mass balance (%)	(ng L^{-1})	(%)	(ng L^{-1})	(%)	(ng L^{-1})	(%)	unfiltered (ng L^{-1})	mass balance (%)	(ng L^{-1})	(%)	(ng L^{-1})	(%)	(ng L^{-1})	(%)
Baptism River	6.8	122.7	1.3	19.7	4.4	64.3	2.6	38.7	0.15	92.9	0.02	14.7	0.07	47.7	0.05	30.5
Baptism River	1.8	*b*	0.1	2.6	*b*	*b*	*b*	*b*	0.13	97.1	0.02	13.5	0.05	34.9	0.06	48.7
Baptism River	12.1	102.9	0.8	6.2	8.5	70.6	3.2	26.1	0.24	94.9	0.04	17.8	0.13	55.2	0.05	21.9
East Creek (headwater)	0.8	*b*	*b*	*b*	*b*	*b*	*b*	*b*	0.29	92.3	0.04	13.7	0.08	28.1	0.15	50.5
East Creek (wetland)	2.6	117.0	0.1	4.2	1.6	61.1	1.3	51.7	0.34	95.3	0.04	11.8	0.21	61.7	0.07	21.8
Everglades (2B south)	6.0	94.5	2.9	48.7	1.0	17.1	1.7	28.7	0.83	100.0	0.62	74.2	0.07	8.4	0.14	17.4
Everglades (3A15)	2.6	75.7	0.0	1.2	0.6	23.5	1.3	51.0	0.22	93.2	0.04	16.5	0.06	28.1	0.11	48.6
Everglades (F1)	8.2	94.3	5.2	63.7	0.9	11.2	1.6	19.4	0.36	87.9	0.24	68.0	0.02	6.6	0.05	13.3
Everglades (U3)	13.1	101.6	8.6	65.3	1.9	14.7	2.8	21.6	0.77	114.3	0.13	17.2	0.28	36.8	0.46	60.3
Fish Creek	0.9	114.7	0.3	31.8	0.1	12.6	0.6	70.3	*c*	*c*	*c*	*c*	*c*	*c*	*c*	*c*
Fish Creek	27.1	96.3	17.5	64.5	6.0	22.2	2.6	9.6	0.12	117.4	0.10	79.5	0.03	25.5	0.01	12.4
Fish Creek	3.7	119.4	1.7	46.9	1.7	45.4	1.0	27.1	0.12	108.5	0.06	46.6	0.04	31.1	0.04	30.8
Hendrie Creek	6.2	96.5	2.4	39.3	0.4	6.8	3.1	50.4	0.13	104.8	0.05	35.4	0.02	18.9	0.07	50.5
Moose River[d]	10.3	100.0	3.1	29.7	4.8	46.5	2.5	23.8	0.86	100.0	0.05	5.3	0.62	71.7	0.20	23.0
Murphy Creek	3.7	98.2	0.5	13.0	0.3	8.8	2.8	76.4	0.21	83.6	0.00	2.3	0.08	37.9	0.09	43.4
Popple River[d]	7.4	*b*	*b*	*b*	*b*	*b*	*b*	*b*	0.62	109.9	0.05	8.2	0.40	64.9	0.23	36.8
Presque Isle River	8.3	114.9	2.0	24.5	5.3	63.3	2.2	27.1	0.14	112.4	0.06	42.1	0.06	43.5	0.04	26.8
Presque Isle River	1.2	127.9	0.2	18.3	0.3	27.5	1.0	82.1	0.08	111.8	0.01	7.9	0.02	29.2	0.06	74.7
Presque Isle River	6.65	117.6	2.8	42.0	3.1	46.9	1.9	28.7	0.12	*c*	*c*	*c*	*c*	*c*	*c*	*c*
Suwanee River	5.9	90.6	1.3	21.4	2.5	42.2	1.6	27.0	0.14	86.0	0.02	13.2	0.06	42.2	0.04	30.6
Tahquamenon River	10.3	99.1	5.4	52.4	2.7	26.5	2.1	20.2	*c*	*c*	*c*	*c*	0.11	*c*	0.09	*c*
Tahquamenon River	2.4	91.7	0.4	16.2	0.9	38.4	0.9	37.1	0.18	97.0	0.04	20.0	0.06	31.1	0.08	45.9
Tahquamenon River	2.92	120.3	1.1	36.6	1.1	37.0	1.4	46.6	0.15	126.6	0.03	21.5	0.08	52.2	0.08	52.9
mean[e]	7.0	104.8	2.9	32.3	2.4	34.3	1.9	38.2	0.30	101.3	0.08	26.5	0.12	37.8	0.10	37.0
SD[e]	5.9	13.6	4.1	20.2	2.3	20.2	0.8	20.1	0.25	11.5	0.14	23.4	0.15	17.5	0.10	16.9
median[e]	6.1	100.8	1.5	30.8	1.6	32.3	1.8	28.7	0.19	98.6	0.04	16.9	0.07	35.9	0.07	33.8
min[e]	0.9	75.5	0.0	1.2	0.1	6.8	0.6	9.6	0.08	83.6	0.00	2.3	0.02	6.6	0.01	12.4
max[e]	27.1	127.9	17.5	65.3	8.5	70.6	3.2	82.1	0.86	126.6	0.62	79.5	0.62	71.7	0.46	74.7

[a] Particulate values were calculated by difference. [b] Total mercury results discarded because mass balance was >130%, filtered value was greater than the unfiltered value, or both. [c] Methylmercury was below detection limit, the filtered value was greater than the unfiltered value, or the unfiltered sample was lost. [d] The filtered fraction was 0.22 μm, not 0.4 μm. [e] Column statistics do not use data from rows that are incomplete.

has been peer reviewed, and our results compare well with other studies.

Suspended particulate matter (SPM) was determined by filtering a known aliquot of water through a preweighed 0.4 μm polycarbonate track-etched filter (Poretics 13028; 47 mm diameter). Uncertainty in the SPM measurement was $\pm$0.09 mg L^{-1} for a typical filter volume of 100 mL. Uncertainty in SPM values above 10 mg L^{-1} was largely due to small filter volumes (<40 mL) and averaged about 2%. Specific conductance and pH were determined using a Hydrolab Scout-2 water quality data system. Specific conductance uncertainty was 1%, and pH uncertainty was $\pm$0.2 pH unit.

Statistical analysis was performed using Minitab version 12.21 for Windows. The normal distribution assumption was tested for each linear regression and *t*-test performed. Linear regression data were tested for departure from normality using the graphical "normal score vs residuals" approach. There was no evidence against the hypothesis that the paired *t*-test data originated from a normal distribution (Anderson−Darling Normality Test; $p \geq 0.18$).

Results and Discussion

The phase distribution of Hg depends in part on the geochemical characteristics of the surface water. Softwater streams with high levels of <0.4 μm filterable organic carbon (OC_F) generally contain more Hg (*24*, *25*), especially within the filtered fraction. This observation has been speculated to result from the presence of colloidal material and has been inferred to mean that the high molecular weight fraction of OC_F plays an important role in regulating the concentration of Hg in natural waters (*24*, *26*, *27*). Use of tangential-flow ultrafiltration in this study allows us to directly quantify colloidal-phase Hg concentrations and to begin to test these suppositions.

Table 1 presents the total concentration and percent organic character of colloids from the broad range of freshwaters in this study. Total colloid concentrations ranged from 0.6 to 58.5 mg L^{-1} of which 50−99.7% was organic matter. Three sites in particular contained a substantial quantity of inorganic colloids: Hendrie Creek (22%), Fish Creek (~40%), and Murphy Creek (58%). Inorganic colloids at Hendrie Creek and Murphy Creek were predominantly iron based. Inorganic colloids at Fish Creek were predominantly aluminum based.

Magnitude of the Colloidal Fraction. Unfiltered Hg_T concentrations presented in Table 2 ranged from 0.9 to 27.1 ng L^{-1} with a median of 6.1 ng L^{-1}, and unfiltered MeHg ranged from 0.08 to 0.86 ng L^{-1} with a median of 0.19 ng L^{-1}. These values were similar to those reported elsewhere for unimpacted freshwaters: 0.1−45.9 ng L^{-1} Hg_T; 0.01−1.77 ng L^{-1} MeHg (*24*, *26*−*30*). Filtered Hg_T concentrations ranged from 0.6 to 11.4 ng L^{-1} with a median of 3.5 ng L^{-1}, and filtered MeHg ranged from 0.02 to 0.81 ng L^{-1} with a median of 0.14 ng L^{-1}.

Colloidal-phase Hg_T concentrations ranged from 0.1 to 8.5 ng L^{-1} with a median of 1.6 ng L^{-1}. Colloidal-phase MeHg concentrations ranged from 0.02 to 0.62 ng L^{-1} with a median of 0.06 ng L^{-1}. As a percentage of the unfiltered value, the colloidal phase contributed roughly 7−72% of both the Hg_T and MeHg load with a median value of 32% Hg_T and 36% MeHg. As a percentage of the filtered value however, the colloidal phase contributed 9−86% of filtered Hg_T and 17−100% of filtered MeHg, with median values of 54.5% and 47%, respectively.

Most published colloidal-phase Hg data has originated from coastal marine environments (*10*, *12*, *14*) where the ionic strength is often more than an order of magnitude higher than freshwaters. In addition, OC_F and Hg concentrations are generally much smaller. Unfiltered Hg concentrations in coastal marine environments have ranged from 0.01 to 9 ng L^{-1} Hg_T and from 0.01 to 0.25 ng L^{-1} MeHg, although Hg_T concentrations as high as 25 ng L^{-1} have been reported in estuaries near the outlet of freshwater rivers (*18*, *29*, *31*−*35*). Filtered Hg concentrations in marine environments ranged from 0.2 to 6.0 ng L^{-1} Hg_T and from 0.06 to 0.09 ng L^{-1} MeHg (*10*, *12*, *14*).

Colloidal-phase Hg concentrations in these studies were also lower than in freshwaters and ranged from 0.04 to 3.48 ng L^{-1} Hg_T and ~0.01 ng L^{-1} MeHg (*10*, *12*, *14*). As a percentage of the filtered fraction, however, the reported colloidal-phase Hg concentrations in freshwater and marine systems were quite similar (Table 3). Note that colloidal-phase data from marine systems were reported for the 0.4 μm−1 kDa range (not 0.4 μm−10 kDa), indicating the importance of low molecular weight compounds in marine systems. Over all, Hg_T and MeHg values ranged from 8% to 93% with means from 32% to 64% for Hg_T and from 16% to 57% for MeHg. The wide range in values likely reflects a number of underlying controls on colloidal-phase partitioning and underscores the need for additional colloidal-phase data to address these process-oriented questions.

A direct comparison of our data to other freshwater investigations is difficult because there are few data available from similar environments, and ultrafiltration protocols vary widely among published studies (Table 3). Freshwater data was available from the Trinity River (*10*, *12*), the Ochlockonee River (*14*), and five sites within the Florida Everglades (*15*) that were located in Water Conservation Area 3, Big Cypress National Reserve, and the Everglades Nutrient Removal Area (shown in Figure 1 as WCA-3, BCNR, and ENR, respectively). One of our four Everglades sites (3A15) was also located within WCA-3, and the rest were located in WCA-2.

Our Everglades data show similar mean phase distributions for both Hg_T and MeHg across all four sites. An average 45% of Hg_T and 44% of MeHg were in the particulate fraction (>0.4 μm); 17% Hg_T and 20% MeHg were in the colloidal fraction (0.4 μm−10 kDa); and 30% Hg_T and 35% MeHg were in the dissolved fraction (<10 kDa). However, our data contrast with Cai et al. (*15*). who found most Hg to be in the smaller size fractions (19% Hg_T and 4% MeHg in the >0.22 μm fraction, 37% Hg_T and 13% MeHg in the 0.22 μm−10 kDa fraction, and 44% Hg_T and 83% MeHg <10 kDa fraction).

Differences in the estimates may result from natural variation in the Everglades (note specific conductance and OC_F differences) but may also result from differences in the ultrafiltration protocol (Table 3). Common to the protocol of both studies were the approximate feed volumes, membrane material, concentration factors (~5), and storage times (processed within ~3 h of collection). Differences include the use of back pressure, the ultrafiltration geometry, the membrane surface area, and the number of fractions retained to complete a mass balance on the separation (2−3 in Cai et al. (*15*) vs 5−7 in this study). We believe low back pressure and a larger membrane surface area reduces membrane fouling and that a rigorous mass balance is important during these early stages of UF evaluation for trace-level research.

Many of the studies in Table 3 report freshwater data using a 1 kDa membrane. In principle, a 1 kDa membrane should provide a better estimate of the truly dissolved phase because the nominal molecular weight limit is closer to the molecular size of aqueous Hg ions. We performed sorption tests on 1 kDa spiral-wound RCL membranes (Millipore PLAC; 0.46 m^2) at neutral pH using a synthetic DOC-free matrix of salts dissolved in prefiltered Milli-Q water. Specific conductance (30 and 1200 μS cm^{-1}), Hg concentration (~6 ng L^{-1} Hg_T and 1 ng L^{-1} MeHg), and pH (~7) were adjusted in that order using high-purity calcium nitrate, methylmercury chloride, mercury(II)nitrate, sodium hydroxide, and nitric acid. At both 30 and 1200 μS cm^{-1}, less than 40% of the Hg

TABLE 3. Comparison with Other Investigations

system	conductivity (μS cm^{-1})	DOC[a] (mg L^{-1})	UF (kDa)	colloidal as % of filtered				feed (L)	material[b]	surface (cm^2)	geometry	applied (psi)	ref
				Hg_T		MeHg							
				range	mean	range	mean						
Coastal Marine Estuary	0.1−36‰	2.6−9.6	1	12−93	57			10−20	PES	9300	hollow fiber	20	(*10*, *12*, *13*)
Trinity River, TX	~200[c]	2.5−6	1	15−53	32			10−20	PES	9300	hollow fiber	20	(*10*, *12*, *13*)
Atlantic Ocean	nr	nr	1	10−43	32			20	PES	4650	cassette	~0	(*14*)
Coastal Marine Estuary	0.3−32‰	2.8−19	1	37−88	67		<2	20	PES	4650	cassette	~0	(*14*)
Coastal Marine Estuary[d]	0.3−32‰	2.8−19	10	12−74	40		<2	20	PES	4650	cassette	~0	(*14*)
Ochlockonee River, FL	~60[e]	12.7	10		76			20	PES	4650	cassette	~0	(*14*)
Everglades	404−602	21.1−27.6	10	28−72	51	8−25	16	10	RCL	177	stirred cell	55	(*15*)
Everglades	239−1189	11.4−34.2	10	23−42	32	17−44	32	5−10	RCL	2300	spiral wound	<4	this study
Midwest OC_C >88%	31−164	1.2−40.7	10	31−85	64	27−76	57	5−10	RCL	2300	spiral wound	<4	this study
Midwest OC_C 50−78%	100−223	0.8−12.7	10	9−86	37	24−100	56	5−10	RCL	2300	spiral wound	<4	this study

[a] The filtered fraction is <0.4 μm except for two sites in the upper Midwest (OC_C > 88%) and the Everglades data from ref *15*, which are both <0.22 μm. [b] RCL, regenerated cellulose; PES, polyethersulfone. nr, not reported. [c] Reported as 0.1‰. [d] 10 kDa data interpolated from Table 1 in ref *14*. [e] Reported as 0.03‰.

feed mass could be recovered. The tests were repeated at pH 5 and pH 9 using metal-complexing buffers (high-purity ammonium acetate and Trizma, respectively). Results improved, but the loss term was still ~50% of the feed. We did not proceed with 1 kDa membranes in freshwaters, but they have been shown to work under marine conditions (*10*). Given the wide range of protocols currently in use (Table 3), an intercomparison between methods is warranted.

Over all, about one-third of the unfiltered Hg_T and MeHg concentration in this study was in each of the three fractions (particulate, colloidal, and dissolved) when averaged across all sites in the investigation (Table 2). To initially assess factors that support colloidal-phase partitioning of Hg in freshwaters, the data set was divided into two groups: One group contained data from sampling dates when the colloidal-phase concentration of Hg comprised >50% of the filtered fraction, and the other group contained data from days when the colloidal-phase Hg concentration was <50% of the filtered fraction. Results from two-sample *t*-tests indicate that SPM load was the weakest indicator of colloidal-phase mercury partitioning (H_o: $\mu_1 = \mu_2$; $p \geq 0.222$ for both Hg_T and MeHg). High DOC was a good indicator for colloidal Hg_T ($p < 0.03$) but not for MeHg ($p = 0.141$). Finally, specific conductance was a strong indicator for both Hg_T and MeHg ($p \leq 0.049$).

Influence of Specific Conductance on the Colloidal Fraction of Hg. Expressed as a percentage of the 0.4 μm filter-passing fraction, the observed colloidal-phase Hg pool decreased as specific conductance increased (open symbols in Figure 2). Ionic strength may influence the observed-phase distribution by at least four mechanisms that are described further below: (1) Ionic strength could change the performance of the membrane by masking the surface charge (an artifact of the separation procedure); (2) it could control the hydrodynamic radius of flexible long-chain colloids (independent of the separation procedure); (3) it could determine the production mechanism and, therefore, control the molecular size of the colloids in the environment (again independent of the separation procedure); and (4) it could promote ion exchange of Hg between functional groups in the colloidal phase and ligands in the "truly" dissolved species (also independent of the procedure).

Membrane performance might change because high concentrations of ions could screen the surface charge on the membrane and allow constituents to pass that would otherwise be sorbed or retained. This hypothesis was tested by performing separations on two types of UF membranes with different surface charge characteristics. Because the magnitude of the surface charge on a regenerated cellulose membrane is larger than that on polyethersulfone (−10.7 and −3.6 mV, respectively (*16*)), one might expect different behavior at low specific conductance (<100 μS cm^{-1}). However, the trend with specific conductance for Hg, a positively charged ion, was similar for both membrane materials (Figure 2, open circles vs open diamonds); the background trend for OC_F, a negatively charged species, was also similar for both membranes (*16*). Therefore, the specific conductance does not appear to change the performance of the membrane, and we infer that the observed trend reflects a true change in the size of the suspended colloids.

The change in the size of colloids with ionic strength could be a function of several mechanisms, including the contraction of long-chain organic material, or differences in the composition of the colloid source material that both covary with ionic strength and determine the molecular size of the colloid (sediment type, for example). Waters that undergo a change in ionic strength, such as the estuarine mixing zone between waters of differing specific conductance, could have ion exchange effects that increase the dissolved-phase concentration by desorbing Hg from the colloidal and particulate phases. This was unlikely with our data because

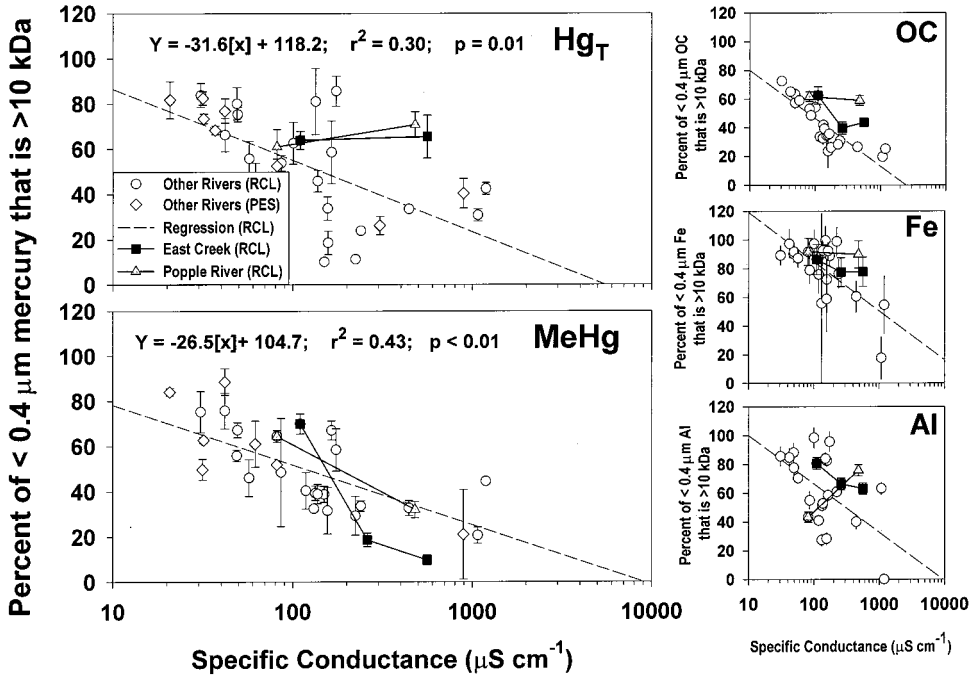

FIGURE 2. Effects of increasing specific conductance of natural samples on the colloidal-phase pool of Hg. For comparison, the colloidal-phase composition at ambient conductance is plotted using open symbols for all rivers in the investigation (circles are data obtained with regenerated cellulose membranes; diamonds are data obtained with polyethersulfone membranes). Samples where conductivity was changed by the addition of $NaNO_3$ or $Ca(NO_3)_2$ are filled symbols connected by a line through the points. The lowest conductance point plotted is the ambient condition of the river. Error bars represent ±1 standard deviation.

there was no concomitant loss in particulate-phase Hg concentration as the ionic strength increased.

To further examine the effect of ionic strength on the observed colloidal-phase distribution and on the sorption and desorption of Hg on colloids, the ambient-phase distribution of the filtered fraction of two high OC_F rivers was compared to the distribution determined on the same source water after increasing the ionic strength. The ambient colloidal-phase composition of each river was roughly equivalent: ~97% organic carbon, ~0.6% aluminum oxides, ~1% iron hydroxides (East Creek Wetland, and Popple River; Table 1).

If the colloidal-phase distribution did not change, we could infer that (1) Hg is associated with colloids whose hydrodynamic radius does not decrease with increasing ionic strength, (2) net ion exchange is minimal, or (3) the kinetics associated with these processes are slow.

The decrease in percent colloidal MeHg with added salts (filled symbols in Figure 2) was similar to the natural trend with specific conductance across all sites (open symbols). However, added salts did not affect the phase distribution of Hg_T. This contrast in behavior suggests a different mechanism of colloidal-phase association for Hg_T than MeHg. Total mercury may be associated with colloidal material that has a hydrodynamic radius that does not contract with increasing ionic strength (inorganic complexes, for example). MeHg appears either strongly associated with colloidal material that contracts (long-chain organic matter) or weakly associated with ligands that are susceptible to ion exchange.

The change with ionic strength in the colloidal-phase distribution of OC_F, Fe_F, and Al_F (surrogates for organic material, insoluble iron hydroxides, and suspended clay, respectively) was consistent with the Hg_T results. At the East Creek, an increasing fraction of OC_C, Fe_C, and Al_C passed through the membrane at higher ionic strength (Figure 2), possibly as a transport vector for MeHg. In contrast, MeHg in the Popple River, likely desorbed from the colloidal phase because OC_C and Fe_C remained constant, and Al_C showed evidence of coagulation from the dissolved phase.

Supporting evidence was also observed in the ratio of MeHg to carbon in the colloidal phase. As the specific conductance was elevated, the MeHg:C ratio decreased for both rivers (from 38 to 5 pg of MeHg/mg of C at East Creek and from 24 to 13 pg of MeHg/mg of C at the Popple River). Coupled with the loss of organic carbon from the colloidal phase observed at East Creek, this suggests that MeHg had a higher affinity for the subset of OC_F that was lost from the colloidal fraction. Coupled with the constant organic carbon percentage at Popple River, this concurs with MeHg loss from the colloidal phase due to ion exchange from weak functional groups on the OC_C.

Although these experiments did not entirely resolve the mechanism behind the observed decline in percent colloidal MeHg, they did suggest several transport vectors from the colloidal to the dissolved phase. The differing partitioning behavior at these sites, despite their similar ambient composition, suggests a coupling between the chemical character of the OC_F and the watershed composition that produced the OC_F. Methods to characterize OC_F are needed to fully interpret these differences because OC_F is not chemically uniform across differing environments. At sites with higher inorganic character in the colloidal phase (Fish, Hendrie, and Murphy Creeks, for example), dissolved organic matter likely coats the inorganic phase. Artificially increasing the ionic strength at these sites may lead to hydrophobically driven coagulation of these mixed composition colloidal particles.

Influence of Dissolved Organic Carbon on the Colloidal Fraction of Hg. Freshwater Hg concentrations in the <0.4 μm fraction have been long correlated to the concentration of OC_F (*24*, *25*, *36*). The regression of Hg against OC_F has generally been stronger for MeHg than for Hg_T. The stronger MeHg regression has been assumed to result from the presence of organic colloids in the <0.4 μm fraction. However,

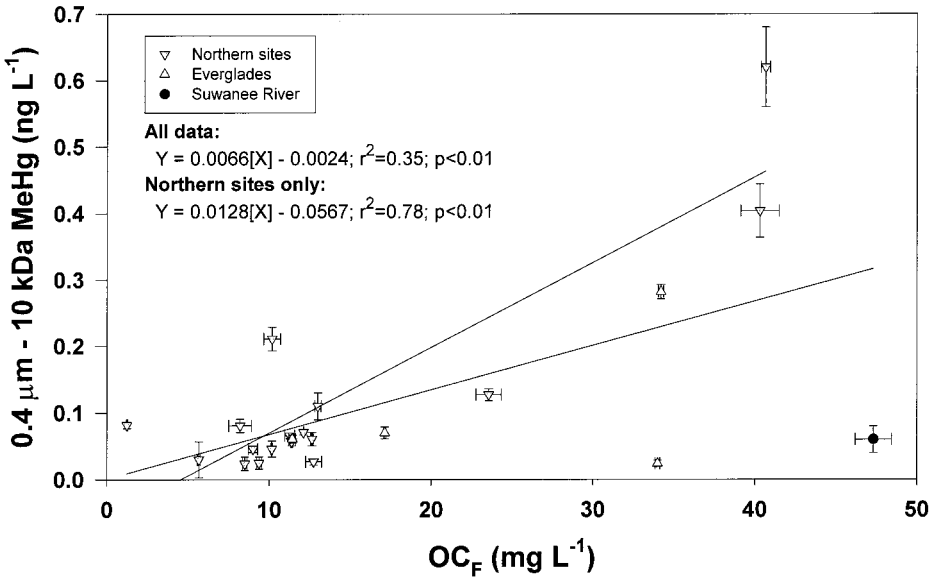

FIGURE 3. Concentration of MeHg in the 0.4 μm−10 kDa fraction as a function of OC_F.

without the tools to isolate the colloidal fraction, a more direct association between MeHg and organic colloids could not be verified. Instead, Hg was shown to be particle reactive, and that quality was assumed to carry into the colloidal size range. Using ultrafiltration, this assumption can be tested.

In this investigation, the correlation between Hg_T and organic carbon within each size fraction and across all size fractions was not statistically significant ($r^2 \leq 0.14$; $p \geq 0.07$). However, MeHg in the colloidal phase and dissolved phase did correlate with the concentration of organic carbon ($MeHg_C = 0.15[OC_C] + 0.0018$, $r^2 = 0.54$, $p < 0.01$; $MeHg_D = 0.006[OC_D] + 0.0458$, $r^2 = 0.23$, $p = 0.02$, respectively). Because ultrafiltration is a difficult and time-consuming technique, the ability to predict the colloidal-phase MeHg concentration from the filtered OC concentration would be advantageous. Unfortunately the regression of $MeHg_C$ with OC_F was not strong when regressed across all sites in the study ($r^2 = 0.35$, $p < 0.01$, Figure 3). It was quite strong within the upper Midwest ($r^2 = 0.78$, $p < 0.01$, Figure 3), but the regression may be biased by relatively few data above 20 mg L^{-1}. Within the Everglades, the regression was poor ($r^2 = 0.18$, $p = 0.58$), and the addition of five data points from Cai et al. (*15*) did not improve the result ($r^2 = 0.15$, $p = 0.34$).

Mercury to carbon ratios in the colloidal phase ranged from 108 to 1142 pg of Hg_T/mg of C (mean = 352 pg mg^{-1}) and from 3 to 205 pg of MeHg/mg of colloidal carbon (mean = 25 pg mg^{-1}). Our Hg:C ratios in the Everglades were about a factor of 2 smaller than that previously published (138−372 pg of Hg_T/mg of C and 4−33 pg of MeHg/mg of C in this study as compared to 301−516 pg of Hg_T/mg of C and 15−52 pg of MeHg/mg of C in Cai et al. (*15*)). That the Hg to carbon ratios were independent of specific conductance argues again that ionic strength controls the concentration but not the quality of organic carbon in the colloidal phase.

There was no significant correlation between Hg:C ratios and ionic strength even when sites were grouped by region (Midwest vs Everglades), by percent organic matter in the colloidal phase (>88% OC_C vs <88% OC_C), or as the entire data set (the p values for the various regressions were ≥0.168). The large range of values in the ratio of Hg to carbon in the colloidal phase indicates site-specific differences in OC_F quality and the resultant partitioning of Hg.

Influence of the Colloidal Phase on Hg Partitioning. On a mass basis, colloidal-phase Hg concentrations ranged from 28 to 338 ng g^{-1} Hg_T (mean = 153; median = 122) and from 1 to 16.4 ng g^{-1} MeHg (mean = 6.6; median = 6.1). The mass basis concentration of MeHg ranged from 0.5% to 25% of the Hg_T value. These values were typical for sediments from unimpacted areas in the Midwest, Ontario, Quebec, and Sweden (9−520 ng g^{-1} (*6*, *37*−*42*) and 0.02−43 ng g^{-1} MeHg, which were 0.1−30% of Hg_T (*6*, *38*, *41*)).

There were no strong trends in Hg concentration (ng g^{-1}) with SPM, conductivity, OC_F, pH, or percent organic character, but MeHg concentration was weakly correlated with conductivity of the riverine water: [MeHg] = 14.6 + 0.0.295-[conductivity] (adjusted $r^2 = 0.21$, $p = 0.03$). Adding additional predictors such as OC_F, SPM, and pH did little to improve the regression.

Partitioning of Hg between the particulate and the dissolved phase is often described using the partitioning coefficient (K_D). Definitions of three partition coefficient models and a table of log K_D values are found in the Supporting Information. In brief, our results show that log K_D for Hg_T ranged from 3.9 to 6.4 with a median of 5.0 and for MeHg ranged from 3.7 to 6.3, again with a median of 5.0.

When 0.4 μm is used as the division between the particulate and the dissolved phase, the filtered fraction may overestimate the truly dissolved phase if colloids are present. This would underestimate K_D and would most likely occur when suspended particulate concentrations are high, because conditions that support an elevated SPM level (high flow, for example) might also elevate colloid concentrations. As a result, when log K_D is plotted against SPM, the slope is often negative (the particle concentration effect (PCE)) (*1*, *23*, *43*).

When SPM concentrations were below 15 mg L^{-1}, data from this study supported the PCE hypothesis. Using the standard division between the particulate and the dissolved phase (0.4 μm), log K_D plotted as a function of SPM showed a weak but significant negative slope ($p \leq 0.01$) for both Hg_T and MeHg. Using 10 kDa as the division, log K_D ranged from 4.3 to 5.5 with a median of 4.9 and for MeHg ranged from 4.4 to 6.2 with a median of 5.0. In addition, log K_D vs SPM showed no significant slope ($p \geq 0.48$) for both species of Hg (Figure 4). Two high SPM points (50 and 236 mg L^{-1} SPM) were excluded from the analysis because they were out of range and had undue influence on the regression. Including both points in the analysis results in regressions that were not statistically significant ($p \geq 0.06$ for both Hg_T and MeHg). As described in Supporting Information, further analysis of K_D indicates that the colloidal mass and not preferential colloidal partitioning drives the PCE.

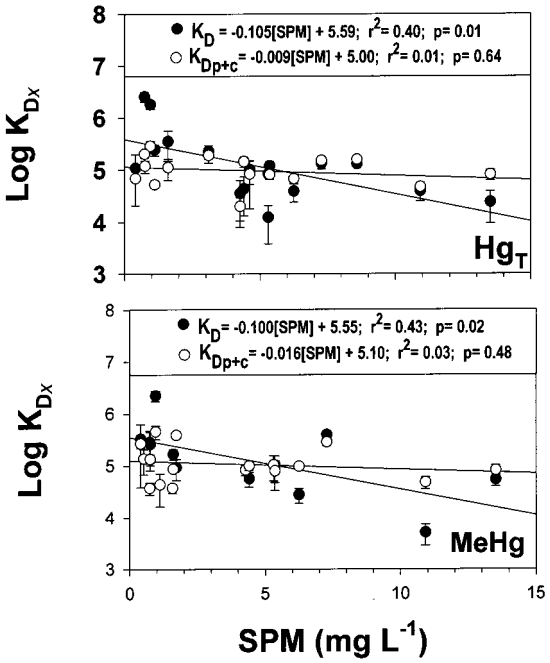

FIGURE 4. Log of the partition coefficient plotted against suspended particulate matter (SPM). K_D (closed circles) indicates a particulate/dissolved cutoff of 0.4 μm, and K_{Dp+c} (open circles) indicates a particulate/dissolved cutoff of 10 kDa. See Supporting Information for mathematical definitions. Two high SPM points (50 and 236 mg L^{-1}) were excluded from the figure because they were out of range and had undue influence on the regression. Including both points in the regression results in p values $\geq$0.06 for both Hg_T and MeHg. Up to two sites for Hg_T and six sites for MeHg were also excluded because their error terms were large (>1 log unit). Excluding these results did not significantly change the results of the regression but did improve the fit of the data to the normal distribution assumption.

Overall, our data demonstrate that the colloidal phase plays an important role in regulating the freshwater partitioning of both Hg_T and MeHg. This result has important implications for the biouptake of Hg and warrants further examination. The colloidal phase must be addressed to thoroughly model the biogeochemical fate and transport of Hg in freshwaters.

Acknowledgments

The authors acknowledge Greg Quinn, Jerry Wegner, Kris Rolfhus, Russ Herrin, Lisa Cleckner, Jennifer Monahan, Robyn Nisi, Jennifer Baeseman, Kymarie Kuster, Shirin Khalili, Jacque Peck, Joel Overdier, and Kou Vang for their assistance in the field and laboratory. We thank three anonymous reviewers of this manuscript for their insight and guidance. This project was funded in part by a grant from the National Science Foundation (EAR-9975444) and by the University of Wisconsin Sea Grant Institute under grants from the National Sea Grant College Program, the National Oceanic and Atmospheric Administration, the U.S. Department of Commerce (Federal Grant NA46RG0481, Project Numbers R/MW-77 and R/MW-80), and from the State of Wisconsin. We also thank David Krabbenhoft and the United States Geological Survey for financial and logistical support from the Aquatic Cycling of Mercury in the Everglades project.

Supporting Information Available

Additional data on OC_D, Fe_D, and Al_D along with our partition coefficient definitions, a table of log K_D values, a comparison to log K_D from other studies, and a graph of the paired t-tests used to determine the importance of the underlying geochemical variables: SPM, OC, and specific conductance. This material is available free of charge via the Internet at http://pubs.acs.org.

Literature Cited

(1) Morel, F. M. M.; Gschwend, P. M. The role of colloids in the partitioning of solutes in natural waters. In *Aquatic Surface Chemistry*; Stumm, W., Ed.; Wiley: New York, 1987; pp 406−422.

(2) Stumm, W.; Morgan, J. Particle−Particle Interaction: Colloids, Coagulation, and Filtration. *Aquatic Chemistry: Chemical Equilibria and Rates in Natural Waters*, 3rd ed.; John Wiley & Sons: New York, 1996; pp 818−871.

(3) Guo, L. D.; Hunt, B. J.; Santschi, P. H.; Ray, S. M. *Environ. Sci. Technol.* **2001**, *35*, 885−893.

(4) Leppard, G.; Burnison, B. Bioavailability: Trace element associations with colloids and an emerging interest in colloidal organic fibrils. In *Trace Element Speciation in Surface Waters and Its Ecological Implications*, 1st ed.; Leppard, G. G., Ed.; Plenum Press: New York, 1983; pp 105−122.

(5) Benoit, J. M.; Gilmour, C. C.; Mason, R. P.; Heyes, A. *Environ. Sci. Technol.* **1999**, *33*, 951−957.

(6) Gilmour, C. C.; Henry, E. A.; Mitchell, R. *Environ. Sci. Technol.* **1992**, *26*, 2281−2287.

(7) Choi, S. C.; Chase, T.; Bartha, R. *Appl. Environ. Microbiol.* **1994**, *60*, 4072−4077.

(8) Hessen, D. O.; Andersen, T.; Lyche, A. *Limnol. Oceanogr.* **1990**, *35*, 84−99.

(9) Tranvik, L. J. *Microb. Ecol.* **1988**, *16*, 311−322.

(10) Wen, L. S.; Stordal, M. C.; Tang, D. G.; Gill, G. A.; Santschi, P. H. *Mar. Chem.* **1996**, *55*, 129−152.

(11) Babiarz, C. L.; Hoffmann, S. R.; Shafer, M. M.; Hurley, J. P.; Andren, A. W.; Armstrong, D. E. *Environ. Sci. Technol.* **2000**, *34*, 3428−3434.

(12) Stordal, M. C.; Gill, G. A.; Wen, L. S.; Santschi, P. H. *Limnol. Oceanogr.* **1996**, *41*, 52−61.

(13) Stordal, M. C.; Santschi, P. H.; Gill, G. A. *Environ. Sci. Technol.* **1996**, *30*, 3335−3340.

(14) Guentzel, J. L.; Powell, R. T.; Landing, W. M.; Mason, R. P. *Mar. Chem.* **1996**, *55*, 177−188.

(15) Cai, Y.; Jaffé, R.; Jones, R. D. *Appl. Geochem.* **1999**, *14*, 395−407.

(16) Hoffmann, S. R.; Shafer, M. M.; Babiarz, C. L.; Armstrong, D. E. *Environ. Sci. Technol.* **2000**, *34*, 3420−3427.

(17) Guo, L. D.; Santschi, P. H. *Mar. Chem.* **1996**, *55*, 113−127.

(18) Gill, G. A.; Fitzgerald, W. F. *Mar. Chem.* **1987**, *20*, 227−243.

(19) Liang, L.; Bloom, N. S. *J. Anal. At. Spectrom.* **1993**, *8*, 591−594.

(20) Liang, L.; Horvat, M.; Bloom, N. S. *Talanta* **1994**, *41*, 371−379.

(21) Bloom, N. *Can. J. Fish. Aquat. Sci.* **1989**, *46*, 1131−1140.

(22) Shafer, M. M. Ph.D. Dissertation, University of Wisconsin, Madison, WI, 1988.

(23) Benoit, G.; Rozan, T. F. *Geochim. Cosmochim. Acta* **1999**, *63*, 113−127.

(24) Hurley, J. P.; Benoit, J. M.; Babiarz, C. L.; Shafer, M. M.; Andren, A. W.; Sullivan, J. R.; Hammond, R.; Webb, D. A. *Environ. Sci. Technol.* **1995**, *29*, 1867−1875.

(25) Mierle, G.; Ingram, R. *Water Air Soil Pollut.* **1991**, *56*, 349−357.

(26) Babiarz, C. L.; Hurley, J. P.; Benoit, J. M.; Shafer, M. M.; Andren, A. W.; Webb, D. A. *Biogeochemistry* **1998**, *41*, 237−257.

(27) Quémerais, B.; Cossa, D.; Rondeau, B.; Pham, T. T.; Fortin, B. *Sci. Total Environ.* **1998**, *213*, 193−201.

(28) Coquery, M.; Cossa, D.; Sanjuan, J. *Mar. Chem.* **1997**, *58*, 213−227.

(29) Benoit, J. M.; Gilmour, C. C.; Mason, R. P.; Riedel, G. S.; Riedel, G. F. *Biogeochemistry* **1998**, *40*, 249−265.

(30) Balogh, S. J.; Meyer, M. L.; Johnson, D. K. *Environ. Sci. Technol.* **1998**, *32*, 456−462.

(31) Mason, R. P.; Fitzgerald, W. F. *Deep-Sea Res. Part I* **1993**, *40*, 1897−1924.

(32) Iverfeldt, Å. *Mar. Chem.* **1988**, *23*, 441−456.

(33) Cossa, D.; Gobeil, C. *Can. J. Fish. Aquat. Sci.* **2000**, *57*, 138−147.

(34) Gill, G. A.; Fitzgerald, W. F. *Deep-Sea Res.* **1985**, *32*, 287−297.

(35) Rolfhus, K. R.; Fitzgerald, W. F. *Geochim. Cosmochim. Acta* **2001**, *65*, 407−418.

(36) Andren, A. W.; Harriss, R. C. *Geochim. Cosmochim. Acta* **1975**, *39*, 1253−1257.

(37) Nater, E. A.; Grigal, D. F. *Nature* **1992**, *358*, 139−141.

(38) Regnell, O.; Ewald, G.; Lord, E. *Limnol. Oceanogr.* **1997**, *42*, 1784−1795.
(39) Grondin, A.; Lucotte, M.; Mucci, A.; Fortin, B. *Can. J. Fish. Aquat. Sci.* **1995**, *52*, 2493−2506.
(40) Gobeil, C.; Cossa, D. *Can. J. Fish. Aquat. Sci.* **1993**, *50*, 1794−1800.
(41) Mucci, A.; Lucotte, M.; Montgomery, S.; Plourde, Y.; Pichet, P.; VanTra, H. *Can. J. Fish. Aquat. Sci.* **1995**, *52*, 2507−2517.
(42) Rossmann, R. *J. Great Lakes Res.* **1999**, *25*, 683−696.
(43) O'Connor, D. J.; Connolly, J. P. *Water Res.* **1980**, *14*, 1517−1526.

Received for review April 25, 2001. Revised manuscript received September 17, 2001. Accepted September 26, 2001.

ES010895V